American Mineralogist, Volume 81, pages 1–8, 1996

The dynamic nature of calcite surfaces in air

S.L.S. Stipp,[1,*] W. Gutmannsbauer,[2] and T. Lehmann[2]

[1] EPFL-DP-IGA, Environmental Surface Analysis Collaboration,
Federal Polytechnical School (DP-IGA, DGR-Ped, DMX-LMCH), and
University of Lausanne (Sci Terre), CH-1015 Lausanne, Switzerland
[2] Institute of Physics, University of Basel, Klingelbergstrasse 82, CH-4056 Basel, Switzerland

Abstract

The {10$\bar{1}$4} surfaces of optical quality calcite (Iceland spar) were examined in air using scanning force microscopy (SFM) immediately after cleavage and during the hours and days that followed. In the absence of a visible contacting solution phase, spontaneous rearrangement of the surface was observed. Images with nanometer-scale resolution showed the formation of hillocks and holes on terraces and cleavage steps; thickness or depth varied from one to ten calcite monolayers (3–30 Å). The rate of surface change varied with geochemical system parameters such as humidity and partial pressure of N_2 and CO_2, but instrument parameters such as imaging force, tip composition, scanning rate, and reimaging frequency had almost no effect. On the basis of previous work documenting the existence of surface-hydration species and a layer of molecular water on samples exposed only to air, we interpret that the observed process results from dissolution and reprecipitation within an invisible layer of water that is adsorbed from air following cleavage. The dynamic nature of calcite surfaces has important implications in conceptual models for the behavior of adsorbed trace metals in unsaturated porous media or arid climates and also for attack on "dry" statues and building stones under acidic atmospheres.

Introduction

Calcite is present in many geologic settings, and its surface structure is important to several processes of interest to environmental geochemistry. As a carbonate mineral, calcite plays a major role in the global CO_2 balance. It is known to take up divalent trace metals and radionuclides from solution, therefore playing a role in contaminant cycling. Because of its moderate solubility, calcite-bearing rocks buffer acid precipitation and acid-mine drainage waters, and several favored building stones (marble, limestone, calcite-cemented sandstone) are vulnerable to destruction in acidic atmospheres.

Very good studies have been published recently about the processes in solution that affect calcite surfaces. Hillner et al. (1992a, 1992b) and Gratz et al. (1993) used scanning force microscopy (SFM) to study dissolution and precipitation in situ at the micrometer scale. Paquette and Reeder (1990, 1995) and Staudt et al. (1994) made significant progress toward explaining preferential sites for metal uptake from solution. Thermodynamic properties in aqueous solutions have been precisely determined (Plummer and Busenberg 1982), and rates of precipitation and dissolution under various conditions have been reported (Nancollas and Reddy 1971; Berner and Morse 1974; Arakaki and Mucci 1995). But what happens to the calcite surface, either freshly fractured or dried after wetting, when it is exposed only to air? Until now, limitations in technology have prevented direct observation at the nanometer scale, and so geoscientists have assumed that in the absence of a contacting solution phase, mineral surfaces remain static.

Molecular-level studies of the uptake of Cd^{2+} (Stipp et al. 1992) and Zn^{2+} (Stipp 1994) by calcite have suggested that some previously undocumented process moves material, that had been adsorbed or precipitated, away from the surface to form a solid-solution under dry conditions. Investigations of calcite surface structure by Stipp and Eggleston (1992), Stipp et al. (1994), and Stipp (1994) revealed the spontaneous development of pits and hillocks on {10$\bar{1}$4} surfaces during exposure only to air. We have been investigating this phenomenon using scanning probe methods, which allow direct observation at the nanometer scale in situ. In this study, we describe the behavior of calcite exposed to controlled atmosphere. Some of the questions we seek to answer are, What is the process? What parameters affect it and how? Can it be the only process responsible for apparent solid-state diffusion of trace metals into bulk calcite? How does this process change our views of the geochemistry of arid and unsaturated systems?

* Permanent address for correspondence: Geological Institute, Copenhagen University, Øster Voldgade 10, DK-1350 Copenhagen K, Denmark.

0003–004X/96/0102–0001$05.00

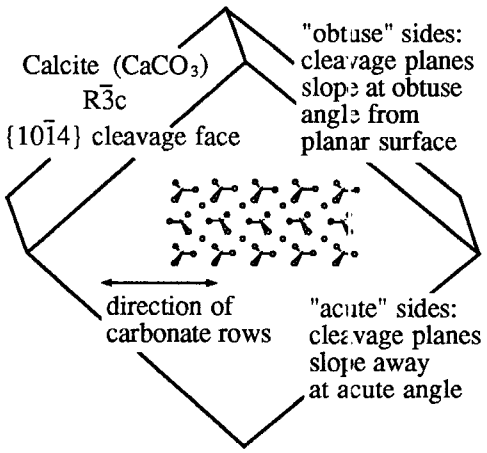

FIGURE 1. A drawing of the cleavage rhombohedron of calcite showing obtuse and acute sides.

MATERIALS AND METHODS

The samples were cleaved just before use from optical quality Iceland spar from Chihuahua, Mexico (Ward Scientific; Siber and Siber). Chemical analyses of several samples by ICP (inductively coupled plasma) indicated that $<1\%$ of Ca sites had been replaced with other metals. The crystals were cleaned with 10% nitric acid made from reagent grade HNO_3 and MilliQ deionized water. After drying, they were cleaved by scratching repeatedly with a scalpel along one of the cleavage directions. This method [described fully in Stipp and Hochella (1991)] produces wide surfaces with few cleavage steps and a minimum of hydrocarbon contamination. Samples were examined from the six faces of single rhombohedra, from different crystals, and from crystals of different locations. The atmosphere was ambient air in most cases; N_2- or CO_2-enriched environments were made in a glove box fitted around the microscope where samples were cleaved during gas flushing. We did not verify partial pressure in the box but assume that final composition was at least 50%. Error in humidity measurements was about $\pm 2\%$. All experiments were conducted at room temperature, 23 ± 4 °C.

Scanning probe microscopy (SPM) is a family of techniques that use a small tip to probe a surface locally. In one design, a sample is scanned in x and y while a laser beam reflects, from the back of the cantilever holding the tip, onto a detector. A record of the movement required in z to maintain constant deflection of the cantilever, and therefore constant force on the tip, is recorded as a normal SFM image; contrast predominantly represents topography. Lateral force microscopy (LFM) is similar except that the detector is also sensitive to cantilever torsion, and so friction coefficients play a major role in image contrast. Noncontact SFM uses a tip that vibrates above the sample. Changes in tip-sample interaction modify the tip's oscillation, and the tip-sample distance is a function of the amplitude. Topography contributes most to contrast in these images, but tip-induced surface modification is less likely. More details about these techniques are found in Meyer (1992) and Güntherodt et al. (1995).

We used three commercial SFM instruments: a Park Scientific Universal, a Digital Nanoscope III, and a TopoMetrix Explorer. Tips were standard Si_3N_4, Si, or gold-coated Si, with spring constants in the range of 0.05–0.25 N/m. Stiffer cantilevers (up to 0.4 N/m) were also tested. In air, determination of absolute imaging force is not possible, even when cantilever spring constants are precisely measured, because of the unknown effects of capillarity. For most image series in this work, scanning force was set as low as possible, at the limit of the repulsive and attractive ranges, so was <10 nN. Scanning rate varied from 0.1 to 3.0 Hz. Optimal scanning size was from 1 to 10 μm square; increased scanning density promoted tip-induced damage. We used 256×256 pixel data collection, and most images were acquired in 3–10 min. Reimaging frequency varied from a few minutes to hours or overnight, and scanning was halted when no images were being collected. The standard tests for imaging artifacts (rotation, scaling, reproducibility on other sites and samples, etc.) were conducted. The images presented here were flattened using a simple polynomial equation to subtract piezoelectric scanner curvature, but no image enhancement or Fourier processing was performed.

OBSERVATIONS AND DISCUSSION

Figure 1 is a diagram of the $\{10\bar{1}4\}$ cleavage surface of calcite showing obtuse and acute sides of the cleavage rhombohedron and the orientation of carbonate rows. A scaled-down version of this diagram is shown as an inset in several figures (e.g., Fig 2a) to indicate orientation, and cleavage direction is marked by a small arrow. Figures 2–7 show several series of images observed under controlled atmosphere. Clearly, the surface changes with time. Imaging (instrumental parameters) and experimental conditions (geochemical system parameters) could affect the rate and character of change.

Figure 3a is a typical image of freshly cleaved calcite. Steps are one to several monolayers high. Terraces are atomically flat. Step edges occasionally follow one of the rhombohedral cleavage planes that intersect the observation plane, but steps formed from both cleavage intersections are rare. Step edges usually indicate the direction from which a sample was cleaved. The shape and direction of cleavage triangles (Figs. 2a, 4a, and 7a) are related to the rate and direction of fracture propagation, as was described by Bethge (1990).

Material mobility and artifacts of imaging

Scanning probe methods are known to be capable of altering surfaces (Güntherodt et al. 1995). Some of the instrument or imaging parameters that might induce movement on any surface are the forces between tip and sample, the tip's contact area, and chemical composition. Scanning rate, scanning density (i.e., image size), and

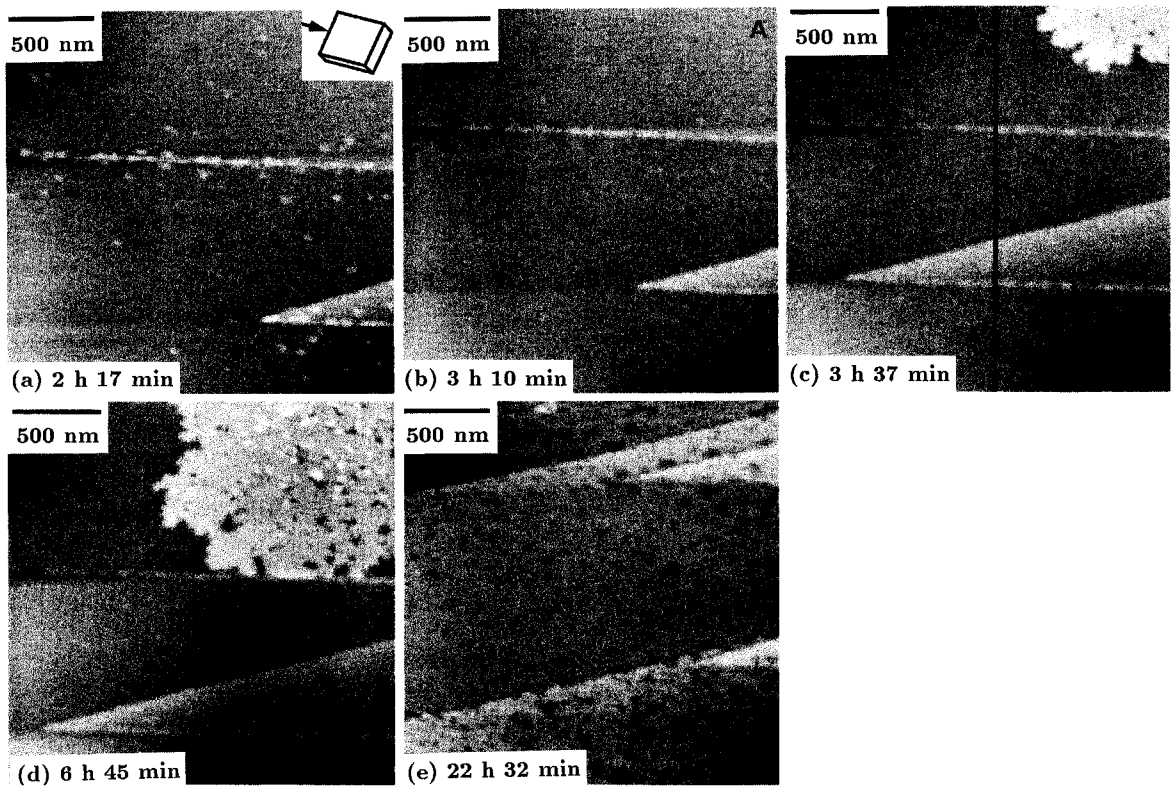

FIGURE 2. A series of SFM images taken from a $\{10\bar{1}4\}$ face of calcite soon after cleavage in air with 30% humidity. Contrast mostly reflects topography: lighter shading represents higher surfaces; darker shading, lower. (**a**) The cleavage triangle (lower right) is one monolayer high (3 Å) and points to the side where cleavage was induced, indicated by the arrow in the orientation sketch, upper right. We notice some nucleation on terraces and directly above the obtuse edges. (**b**) Hillock height decreases. (**c**) Displacement of scanning area to the right shows that height decrease of hillocks is not an artifact of frequent scanning because the spots have similar appearance on the never-scanned region, right of the vertical line. An area of rapid accumulation appears in the top right corner. (**d**) Rapid accumulation is halted by a step down. (**e**) This image was taken the next day from a site near **d**. A thick layer (12 Å) covers each terrace. Holes extend to the original material, but height difference between terraces is conserved as one monolayer.

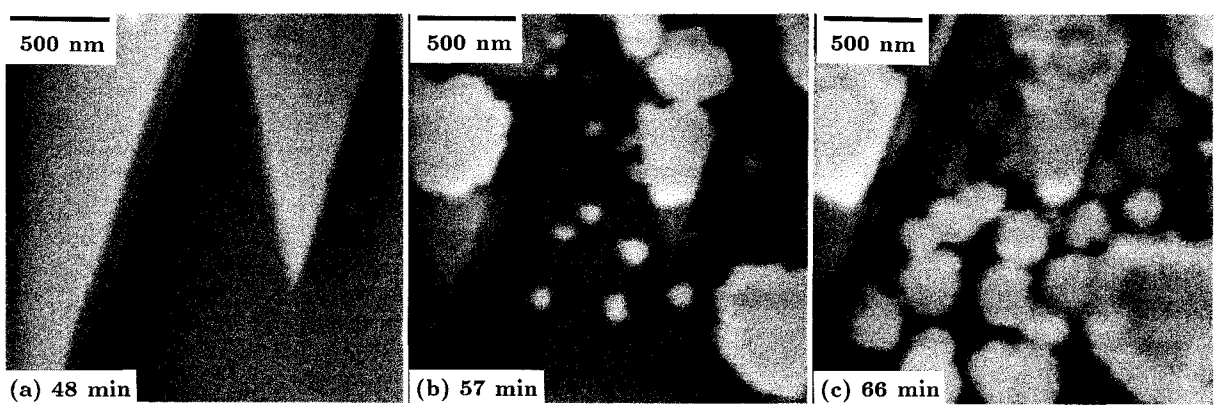

FIGURE 3. SFM in air with 30% humidity. The shadows beside high-relief areas on this and other images are artifacts of the software, which adjusts for piezo-scanner curvature. (**a**) Atomically flat terraces with height of one to two monolayers. Surface remains static for about 50 min through several scans. Suddenly, rapid accumulation begins (**b**), extends (**c**), and covers the entire area within 27 min (not shown). Notice the growth zoning and straight edges on some parts of the flowers.

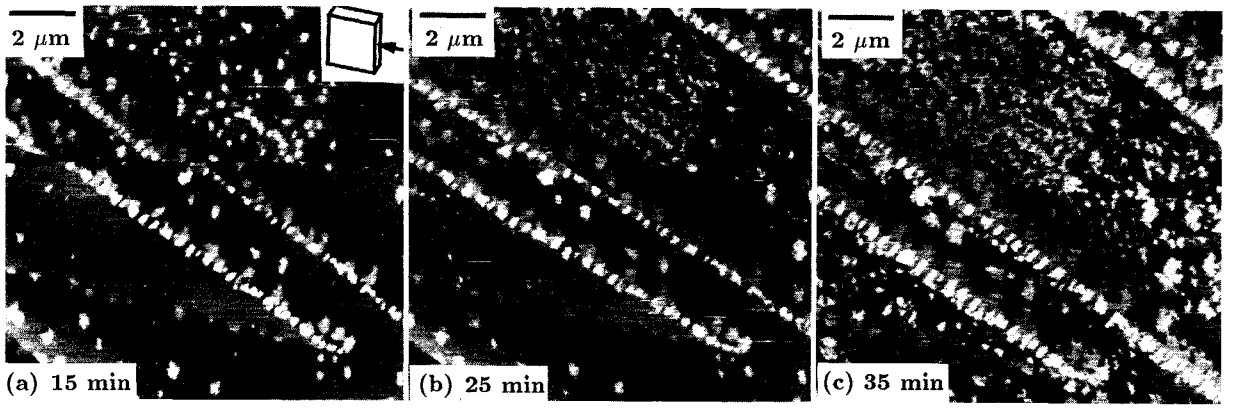

FIGURE 4. SFM in air with >50% humidity. In a, the large arrow marks a change in the scanning direction, a test for artifacts. These images show well-behaved accumulation. Notice holes oriented in one direction and outgrowth normal to step edges. The small arrow in a points to an example of step-edge erosion.

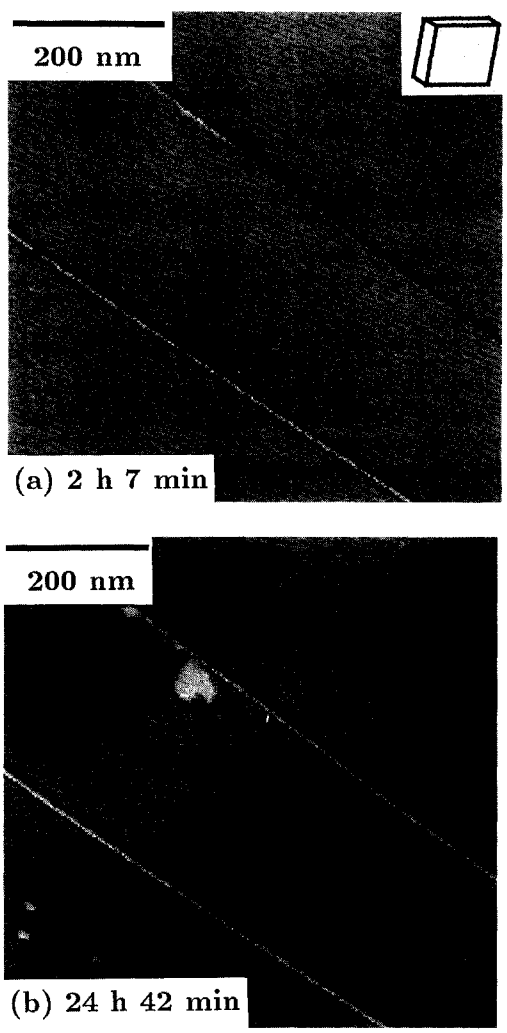

FIGURE 5. LFM in air with ≅5% humidity. Contrast is mainly from differing friction coefficients. Lower humidity inhibits rearrangement.

reimaging frequency might affect material buildup or removal. In general, we did not observe significant, consistent correlation between surface behavior and most of these instrument parameters.

There were no significant differences in images taken with tips made of Si_3N_4, Si, or gold-coated Si, but this was expected. Gold coating is easily torn off (unpublished results), exposing Si, and surfaces of both Si and Si_3N_4 tips are known to oxidize to SiO_2 with air exposure. Although Si tips are manufactured to be sharper, so depending on capillary forces might have a lower contact area and higher pressure on the sample, work in our laboratory indicates that tips often break or collect surface dust. Therefore, true tip-sample contact area is not simply related to tip composition. Changing the force by an order of ±10 from the usual working range at the limit between attractive- and repulsive-mode contact imaging had no effect; however, increasing the force to higher levels in repulsive mode (stiffer tip, more deflection) induced scraping of both accumulated and original material. When imaging force was minimized, scanning rate, scanning density, and reimaging frequency had no effect on the images.

To test whether the tip was responsible for surface rearrangement, some images were collected using noncontact mode. Figure 6 shows the development of both holes and hillocks; their size and distribution change with time, though tip-surface interaction was minimized. Figure 2 shows the results of another test. A particular region was sequentially scanned (four times) in contact mode with net force set near zero. Spots that had previously accumulated appeared to decrease in height (compare Fig. 2a with Fig. 2b). Displacement of the scanning area by about 1 μm (Fig. 2c) showed a never-scanned zone (right of vertical line) where spots were not significantly different than on the frequently scanned side (left). This suggests the tip was not responsible for loss of material. Other tests were conducted in which samples were electronically and mechanically rotated to see whether scanning direction changed the pre-

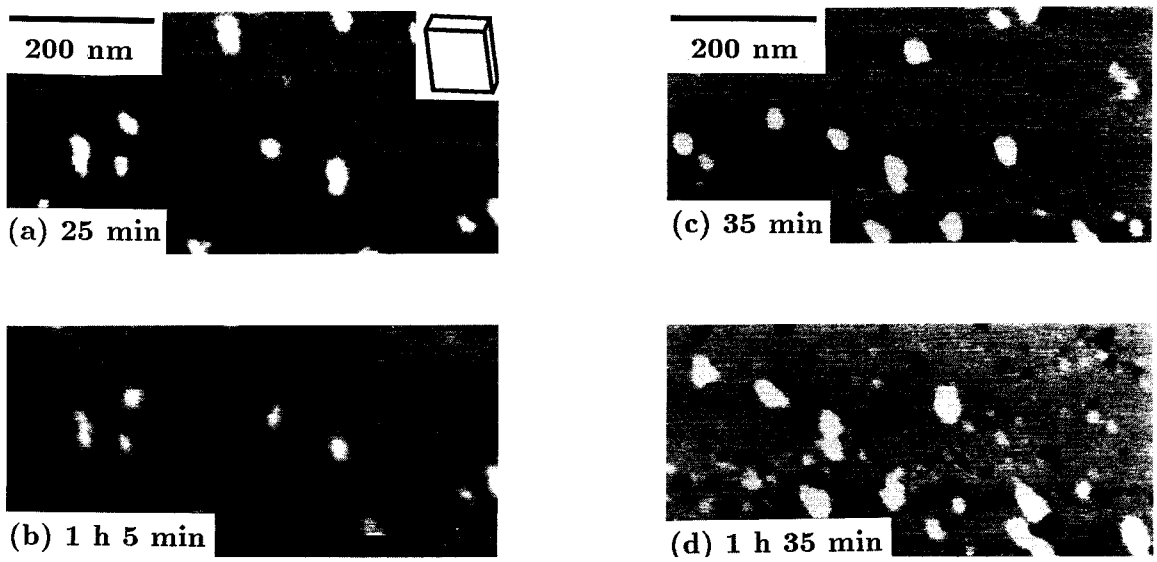

FIGURE 6. Series of images taken from one site using noncontact mode in air with ~40% humidity. Both hillocks and holes developed and disappeared, as shown by arrows. Some time-dependent drift affected the scanning location. Images **a** and **b** show the same site with a time lapse of 40 min, whereas **c** and **d** show a site a fraction of a micrometer away during an overlapping time interval.

ferred orientation of hills or holes. It did not. Images from series in which scanning was almost continuous were not significantly different from images of adjacent areas that were scanned only once or twice in 24 h. These results prove that mobility of material is not limited to regions of contact with the tip; however, they do not prove that imaging has no effect on material mobility.

Material mobility and geochemical system parameters

Changes in system parameters had a significant effect on surface behavior. Comparison of Figures 4 and 5 shows the difference in mobility during exposure to 50 and 5% relative humidity, respectively. The partial pressure of CO_2 also had an effect, as expected from carbonate equilibria. Underlying crystal structure seems to influence the number, location, and direction of growth of both holes and hillocks. Some areas have more nucleation sites than others. Compare the hole density on the three terraces of Figure 2e. In Figure 4b, the number of growth spots varies on a single terrace (under the scale bar). Surface character is discussed more below, but there is as much variability in appearance among several sites on the same sample, or among several samples cut with the same crystallographic orientation from the same crystal, as there is among differently oriented faces from the same crystal, or among samples from different locations. For this reason, a macroscopic rate constant for surface mobility is difficult to define from the images. Rate of change decreases with age, but material recently accumulated often disappears again. Compare Figure 7b with Figure 7c and Figure 2a with Figure 2b.

Sample history also affects surface appearance. Samples exposed to solution at equilibrium with atmospheric CO_2 and calcite, and then dried, tend to develop more holes and blurring of features during exposure to air (Stipp et al. 1994); however, freshly fractured surfaces appear to accumulate material. This can probably be explained because fractured surfaces, even when swept with a nitrogen stream, still have small particles of calcite dust physically clinging, that are gone after exposure to solution. Ostwald ripening, the in-solution process by which small crystals are consumed for the growth of larger ones, suggests that decrease in surface free energy favors recrystallization of dust particles onto larger surfaces. The observed phenomenon of spontaneous surface mobility seems to be an example of dynamic equilibrium but apparently occurs without the aid of solution in contact. We return to this point later.

The material

The evidence collected so far cannot prove conclusively whether the accumulating mineral is or is not calcite. Alignment of hillocks and holes perpendicular to step edges and along crystallographic directions suggests epitaxial accumulation over the original surface. Well-behaved growth results in step heights that are consistently multiples of about 3 Å, the height of the calcite $\{10\bar{1}4\}$ monolayer. We observed nanometer-scale holes in the accumulated material, so we might suppose there are also molecular-scale holes and defects. This would result in a density difference between accumulated and original material and a slight difference in some physical properties. Lateral force images (such as Fig. 5) do indicate a different contrast for the accumulated material, but deconvolution of forces responsible for image contrast is not straightforward when the contrasting area is also consistently topographically higher. Clearly, more work is need-

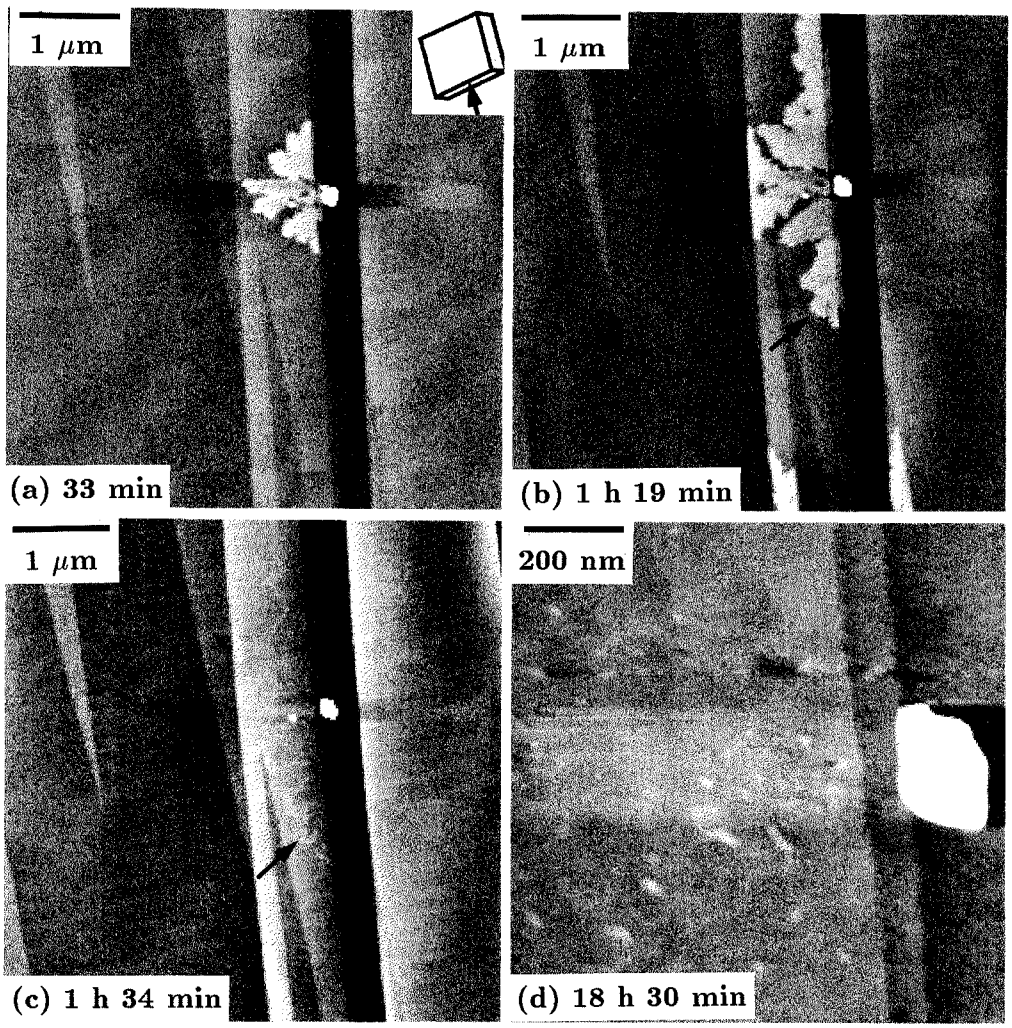

FIGURE 7. Air with 30% humidity. (**a** and **b**) A calcite particle about 130 Å and 200 nm wide clings to a step edge. Material (18 Å high) spreads out from it symmetrically to a line perpendicular to the step edge. (**c**) Accumulated material disappears again leaving the original dust particle and a faint trace along the lower edges of what were the "angel wings." (**d**) The next morning (note changed scale), holes (one to three monolayers) and remnant hillocks (one monolayer) are left. The particle shape is rhombohedral.

ed to determine the structure of the accumulated material.

The mobilized material comes from holes (Fig. 6) and step edges (Fig. 4a, small arrow), and mostly from dust left after cleavage. Even after sweeping the surface with pressurized N_2, some small particles of calcite remained clinging to the surface, and we observed layers of material spreading from them (e.g., Fig. 7).

There are four categories of surface behavior. We have not yet defined the geochemical system parameters that control the development of one type of mobility and accumulation over others, and indeed several types can be found within the same scanned area or in different areas of the same sample. Classification simply serves to organize the observations and lead toward an understanding of the process.

Outgrowth from a step. This type of growth appears well behaved. It spreads one layer at a time, as we see in Figure 4 and less clearly in Figure 2a, preferentially from obtuse, rather than acute edges. A difference in dissolution and metal uptake behavior on obtuse and acute edges has been previously reported (Stipp and Eggleston 1992; Hillner et al. 1992a, 1992b; Staudt et al. 1994; Paquette and Reeder 1995). Cross sections show new material to be about 3.0 Å, one monolayer high. Growth usually occurs perpendicular to step edges in tongues with fractal aspects; edges roughly parallel cleavage directions (Fig. 4). Sometimes, rather than outgrowth at steps, holes form adjacent to step edges into the terrace beneath, as rounded rhombohedral pits about three to six monolayers deep.

Decoration on top of steps. On some samples, deco-

rations form, spaced along the top of obtuse step edges (Figs. 4a and 2a). They are usually one monolayer high and elongated in one dimension. Their formation seems to be impeded by or impedes the outgrowth of steps, and so decorations alternate with step outgrowths (Figs. 4 and 2a).

Nucleation of hillocks and holes on terraces. Both holes and hillocks nucleate and grow on the middle of terraces, but their densities vary (Fig. 4b). Often, holes elongate in one direction and hillocks in another (Fig. 6d). Height and depth are usually one to three monolayers during formation, but the holes and hillocks may grow or disappear again.

Rapid accumulation of material. In comparison, this growth is less ordered but is frequently symmetric, and edges and hole boundaries are sometimes straight and aligned along crystallographic directions. Figure 3 shows three images from a sequence where a fresh surface became completely covered within 30 min. The flowers even show growth banding. Rapidly accumulated material is often many monolayers (four to ten) high, in contrast to types discussed above, and covers terraces completely. Often holes remain, extending to the original surface, and the number of holes varies. Although a new layer is much higher than one step by itself, it has trouble moving up or down over step edges (Fig. 2d), and when it does spread over, it prefers obtuse edges. Most often, material accumulates and covers each terrace independently, but two adjacent terraces, separated by a one-monolayer step, may each be covered by layers that are four monolayers thick, so the final step difference is conserved as one monolayer (Fig. 2e). In some cases, accumulated material rapidly disappears again, and holes form on the original surface beneath (Figs. 7c and 7d).

The process

These dynamic surface changes have many similarities with behavior predicted by theories for crystal growth in solution or melt. However, thermodynamics predicts that surface diffusion is not energetically favored for an ionic solid. On the termination of the bulk structure, energy thresholds are simply too great for an ion to overcome its bonds in a site surrounded by opposite charge, which hold it back, and move past ions of similar charge, which repel it, to a new site.

A solution to this problem is found in evidence from other studies. We know that calcite surfaces are hydrated and that strongly bonded hydrolysis species, $S{\cdot}CO_3H$ and $S{\cdot}CaOH$ (where $S{\cdot}$ represents the calcite surface), are present on surfaces cleaved in air even after exposure to ultra-high vacuum (Stipp and Hochella 1991). Thus, dangling bonds are satisfied, and the threshold resulting from differentially charged surface sites is not as high in reality as on a theoretical termination of the bulk structure. In addition, we know that all surfaces in air are covered by a capillary layer of water. This is evident from the forces that affect tip approach with SFM (Cleveland et al. 1995) and from experiments using synchrotron X-ray reflectivity. Chiarello et al. (1993) showed that in one case, there was a layer of "water" at least 20 monolayers thick on calcite in air. From macroscopic studies, we know that calcite has moderate solubility and that rates of dissolution and recrystallization are relatively fast, so we can assume that the water layer quickly becomes a layer of solution saturated with respect to calcite and the contacting CO_2 partial pressure. SFM reveals evidence of mobility as early as 10 min after fracture when relative humidity is 30% or more (room temperature, atmospheric CO_2). Our observations suggest that the wetted calcite surface reduces its surface free energy by mass rearrangement within the invisible layer of water, and with SFM we can watch it.

Whether this process is sufficient, by itself, to explain the apparent solid-state diffusion of Cd^{2+} and Zn^{2+} from surface layers into the bulk, as was reported by Stipp et al. (1992) and Stipp (1994) remains to be shown. The overlayer of $CdCO_3$ that was grown on calcite was at least 30 monolayers thick, and exchange of metal ions occurred within several weeks under ultra-high vacuum conditions. In the experiments reported here, we did not see evidence that rearrangement goes to such a depth.

Implications

Because the dissolution and precipitation kinetics of calcite are neither too fast nor too slow, we are able to see aspects of crystal growth in situ at micrometer to subnanometer scale. This has provided an opportunity to verify macroscopic properties and test our conceptual models for molecular-level behavior. On a more practical level, these results show that our current assumptions regarding surfaces of calcite, and probably other carbonate minerals, in dry environments need revising. The surface does not remain static but is highly dynamic. Calcite in soil or sediment, which serves as an adsorbent for trace metals from groundwater, recrystallizes with them as a solid solution under wet conditions. Now we see that rearrangement also takes place on "dry" surfaces, thus liberating adsorption sites for more uptake during the next exposure to solution and substantially increasing uptake capacity of calcite for structurally compatible toxic metals and radionuclides. For building stones, statues, and terrains exposed to acidic atmosphere, the solution layer is at equilibrium with the CO_2, NO_x, and SO_2 in contact. Thus, acid attack is not limited to rainfall events but is instead continuous.

Acknowledgments

Many people helped to make this study possible. Warmest appreciation goes to Andrzej Kulik and Carrick Eggleston for providing access to their instruments. Sincere gratitude for interest and support goes to members of the Environmental Surface Analysis Collaboration, Lausanne, including Willy Benoit, Andrzej Kulik of Inst. Génie Atomique, Jean-Claude Védy of Dépt. Génie Rural, and Hans-Jürg Mathieu of Lab. Chimie Métallurgique, all of Ecole Polytechnique Fédérale; Hans-Rudolf Pfeifer, Philippe Thélin, and Johannes Hunziker of Dépt. Sciences de la Terre, Uni-

versité de Lausanne; and Hans-Joachim Güntherodt and his group at Physics Inst., University of Basel, Switzerland. The work was improved by discussions with Lukas Eng, Nancy Burnham, and Pierre-Jean Gallo, and we appreciate comments by Patricia Maurice, Dirk Bosbach, and two anonymous reviewers.

References cited

Arakaki, T., and Mucci, A. (1995) A continuous and mechanistic representation of calcite reaction-controlled kinetics in dilute solutions at 25°C and 1 atm total pressure. Aquatic Geochemistry, 1, 105–130.

Berner, R.A., and Morse, J.W. (1974) Dissolution kinetics of calcium carbonate in sea water: IV. Theory of calcite dissolution. American Journal of Science, 274, 108–134.

Bethge, H. (1990) Molecular kinetics on steps. In M.G. Lagally, Ed., Kinetics of ordering and growth at surfaces, p. 125–144. Plenum, New York.

Chiarello, R.P., Wogelius, R.A., and Sturchio, N.C. (1993) In-situ synchrotron X-ray reflectivity measurements at the calcite-water interface. Geochimica et Cosmochimica Acta, 57, 4103–4110.

Cleveland, J., Shaffer, G., and Hansma, P.K. (1995) Hopping between water layers on calcite with AFM. Physics Review Letters B, in press.

Gratz, A.J., Hillner, P.E., and Hansma, P.K. (1993) Step dynamics and spiral growth on calcite. Geochimica et Cosmochimica Acta, 57, 491–495.

Güntherodt, H.-J., Anselmetti, D., and Meyer, E. (1995) Forces in scanning probe methods. Nato ASI Series E, Applied Sciences, Vol. 286, Schluchsee, Black Forest, Germany, March 7–18, 1994.

Hillner, P.E., Manne, S., Gratz, A.J., and Hansma, P.K. (1992a) AFM images of dissolution and growth on a calcite crystal. Ultramicroscopy, 42–44, 1387–1393.

Hillner, P.E., Gratz, A.J., Manne, S., and Hansma, P.K. (1992b) Atomic-scale imaging of calcite growth and dissolution in real time. Geology, 20, 359–362.

Meyer, E. (1992) Atomic force microscopy. Progress in Surface Science, 41, 3–49.

Nancollas, G.H., and Reddy, M.M. (1971) The crystallization of calcium carbonate: II. Calcite growth mechanism. Journal of Colloid and Interface Science, 37, 824–830.

Paquette, J., and Reeder, R.J. (1990) New type of compositional zoning in calcite: Insights into crystal-growth mechanisms. Geology, 18, 1244–1247.

——— (1995) Relationship between surface structure, growth mechanism, and trace element incorporation in calcite. Geochimica et Cosmochimica Acta, 59, 735–749.

Plummer, L.N., and Busenberg, E. (1982) The solubilities of calcite, aragonite, and vaterite in CO_2-H_2O solutions between 0 and 90°C, and an evaluation of the aqueous model for the system $CaCO_3$-CO_2-H_2O. Geochimica et Cosmochimica Acta, 46, 1011–1040.

Staudt, W.J., Reeder, R.J., and Schoonen, M.A.A. (1994) Surface structural controls on compositional zoning of SO_4^{2-} and SeO_4^{2-} in synthetic calcite single crystals. Geochimica et Cosmochimica Acta, 58, 2087–2098.

Stipp, S.L.S. (1994) Understanding interface processes and their role in the mobility of contaminants in the geosphere: The use of surface sensitive techniques. Eclogae Geologicae Helvetiae, 87, 335–355.

Stipp, S.L., and Hochella, M.F., Jr. (1991) Structure and bonding environments at the calcite surface as observed with X-ray photoelectron spectroscopy (XPS) and low energy electron diffraction (LEED). Geochimica et Cosmochimica Acta, 55, 1723–1736.

Stipp, S.L.S., and Eggleston, C.M. (1992) Calcite surface structure observed with scanning force microscopy (SFM). American Chemical Society Meeting, Geochemical Section Abstracts, Symposium for Mineral Surfaces. San Francisco, California, April 5–10, 1992.

Stipp, S.L., Hochella, M.F., Jr., Parks, G.A., and Leckie, J.O. (1992) Cd^{2+} uptake by calcite, solid-state diffusion and the formation of solid-solution: Interface processes observed with near-surface sensitive techniques (XPS, LEED, and AES). Geochimica et Cosmochimica Acta, 56, 1941–1954.

Stipp, S.L.S., Eggleston, C.M., and Nielsen, B.S. (1994) Calcite surface structure observed at microtopographic and molecular scales with atomic force microscopy (AFM). Geochimica et Cosmochimica Acta 58, 3023–3033.

Manuscript received July 26, 1995
Manuscript accepted October 6, 1995